The *ARL Monopod II* Running Robot: Control and Energetics

M. Ahmadi and M. Buehler, `http://www.cim.mcgill.ca/~arlweb`
Center for Intelligent Machines, McGill University, QC H3A 2A7, Canada

Abstract

This paper presents the experimental implementation of an energy efficient "Controlled Passive Dynamic Running" strategy (CPDR) on a planar one-legged running robot with hip and leg compliance. The approach was introduced via simulations in [1], and tested via preliminary experiments [2]. The improved version described here permits running speed of up to $4.5km/h$ *with a total mechanical power expenditure of only* $48W$*, which translates into a specific resistance of only* 0.22*. This is the highest efficiency among all actively controlled legged robots.*

1 Introduction

Energy autonomy, and thus high energy efficiency is a necessity for virtually any practical mobile robot. This can be particularly challenging in legged robots, since a great deal of energy might be expended for internal motions which do not directly contribute to positive work in the direction of motion, such as maintaining vertical body oscillations or simply swinging the legs. One way to minimize this energy expenditure is to use a mechanical design which provides much of the needed limb motion as its "passive dynamics," that is, without actuation at all. Many animals exploit passive dynamics, and manage to reduce the metabolic cost of running by utilizing the elastic properties of their muscles, tendons, and bones [3]. The same principle is at work during human locomotion: the leg and body work as an inverted pendulum in walking, and as a mass-spring system (together with the muscle elasticity) in running.

Raibert [4], after work by Matsuoka [5], pioneered the use of a spring-mass system's unforced response, its "passive dynamics," to generate the gross vertical oscillatory motion for hopping robots. To date, virtually all dynamically stable running robots utilize a spring-mass system to provide the vertical robot motion [4, 6, 7, 8]. A beautiful example of just how far the passive dynamics approach can be carried was provided by McGeer [9] who built a two legged walking robot with knees which walked down a shallow incline driven entirely by gravity.

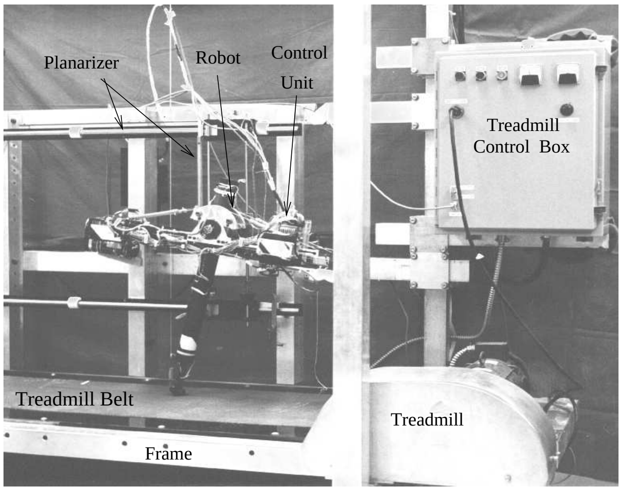

Figure 1: *Experimental setup*

The experiments reported in [7] showed that the ARL Monopod I (without hip compliance) expended 40% of the total energy requirement for running at its top speed of $4.3km/h$ for simply swinging the leg. Much of this energy can be saved, since passive dynamics can provide the leg swing motion via a spring connecting the leg and the body at the hip joint as proposed in [10]. In our previous work [1], we presented a new control strategy to stabilize passive dynamic running (CPDR) of a one-legged robot called. Preliminary experiments with the ARL Monopod II were reported in [2]. In this paper we present the full implementation of the control strategy, report greatly improved performance, and discuss the resulting energetic performance in detail.

2 ARL Monopod II

The ARL Monopod II (Figure 1) consists of a body connected to a prismatic leg at the hip joint, and is constrained to move in a vertical plane. It is about

$0.7m$ tall and weighs $18kg$. The system has a total of seven degrees of freedom (Figure 2), including the leg length (r), leg actuator displacement (p_l), hip actuator displacement (p_h), leg angle (θ), and three degrees of freedom of the body (x, z, ϕ). Due to kinematic constraints, not all of them are free simultaneously. During stance there are five degrees of freedom $(r, \theta, \phi, p_h, p_l)$, and during flight there are six $(x, z, \theta, \phi, p_h, p_l)$. Both the hip and leg actuators are connected in series with the springs. The actuator inputs are the hip and leg motor torques, τ_h and τ_l. The robot parameters can be found in [11, 2] and are omitted here for brevity.

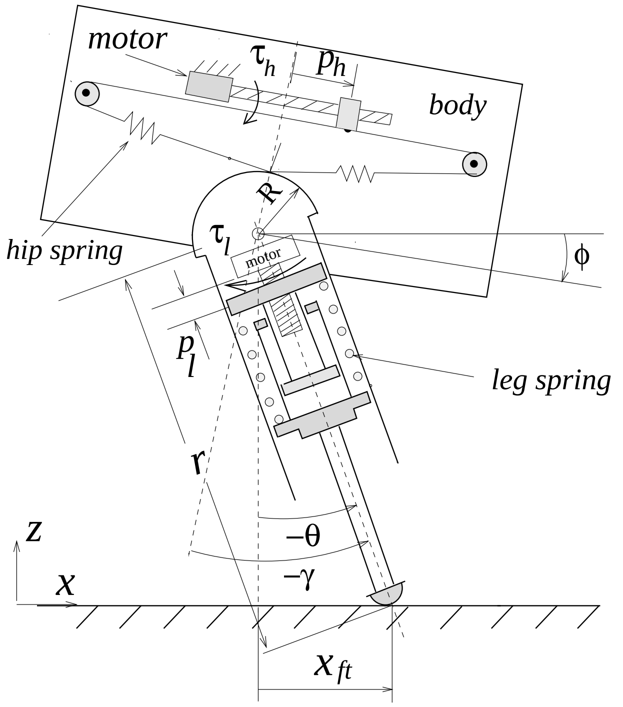

Figure 2: *ARL Monopod II with important variables.*

For this robot, running is a combination of two synchronized oscillations: the vertical hopping motion of the robot over the leg spring, and the counter-oscillations of the leg and body about the hip via the hip spring. With proper initial conditions, the robot can hop for a few steps completely unactuated, before it falls. This running motion is unstable, but is produced entirely by the robot's passive dynamics. It can be stabilized via minimal actuator effort to compensate for the losses and errors. The CPDR strategy [1] calculates the ideal passive joint trajectories for any given forward speed and uses them as the nominal input reference trajectories to the joint controllers for tracking.

3 Control

The two main tasks of the controller are hopping height control and planar motion control. The planar motion controller controls the forward speed at the top level, and the leg and body angles at the joint level. The two control tasks are synchronized by expressing the trajectories in terms of "Locomotion Time."

3.1 Hopping Height Control

The objective is to achieve the desired apex height during flight while the vertical thrust is only available during stance. How should an apex height error, only available once per robot step, translate into a torque command which only acts during the next stance? A new energy based controller during stance overcomes this problem.

We define the "vertical energy" as the total energy when the robot is allowed to move only along a vertical line. It can be expressed as

$$E_v = E_{pot} + E_{kin,v}$$

where E_{pot} is the gravitational and leg spring potential energy, and $E_{kin,v}$ the kinetic energy. If we assume that the leg actuator settles to its desired value before apex height, there will be a one-to-one correspondence between the apex energy, E_{apex}, and the apex height, z_{apex}. Therefore, the hopping height and the apex energy control problems are equivalent. For any given desired height $z_{apex,d}$, the controller has to regulate E_v to the corresponding desired value of $E_{apex,d}$. This is a much simpler task than direct control of the hopping height due to its independence from touchdown and lift-off heights.

A new *adaptive energy feedback controller* is used as follows. Consider two consecutive steps, where each step is defined to start at one apex and to end at the next one, and the vertical energy of the robot at the n_{th} apex is E^n_{apex}. The energy at the next step E^{n+1}_{apex}, is a function of the the current apex energy, E^n_{apex}, the added energy by the actuator during the n_{th} step, E^n_{act}, and the energy lost during the same step,

$$E^{n+1}_{apex} = E^n_{apex} + E^n_{act} - E^n_{loss}.$$

The objective of the controller is to make $E^{n+1}_{apex} = E_{apex,d}$. While E^n_{loss} cannot not be measured before the corresponding step finishes, an estimate $\tilde{E}^n_{loss}$, can be used to find the desired actuator energy as

$$E^n_{act,d} = E_{apex,d} - E^n_{apex} + \tilde{E}^n_{loss}.$$

The following simple model is used for estimation

$$\tilde{E}^n_{loss} = K^n_{loss}(E^n_{apex} - E_0),$$

where K^n_{loss} is the only model parameter to be updated via

$$K^{n+1}_{loss} = K^n_{loss} + \frac{1}{2}\frac{E_{apex,d} - E^{n+1}_{apex}}{E^n_{apex} - E_0},$$

and E_0 is a constant which depends on the potential energy reference.

The energy added by the leg actuator can be measured via $E_{act}(t) = \int_{t_{td}}^{t} F_l \dot{p}_l dt$, where F_l is the leg force, $\dot{p}_l$ is the actuator velocity and t_{td} is the touchdown time. A simple leg actuator velocity controller is used to add or remove energy from the system. Hence, the desired velocity should be a function of the added energy error

$$\dot{p}_{l,d} = \psi(E^n_{act,d} - E_{act}(t)),$$

where ψ is a shaping function to prevent actuator saturation at touchdown. ψ is zero at touchdown and lift-off and peaks when the spring is fully compressed. This energy controller is combined with an on-line offset error estimation and compensation resulting in a very accurate control of the energy (and thus apex height) as shown in Figure 5. This accuracy is important in the stability of the algorithm.

3.2 Planar Running Control

Locomotion Time: It serves to synchronize the leg-body oscillation to the vertical motion by re-scaling time such that stance and flight times are always mapped onto a fixed interval on the real line. We selected the flight and stance locomotion times,η_f and η_s, as

$$\begin{aligned} \eta_f = & \quad \tfrac{2\dot{z}-(\dot{z}_{td}+\dot{z}_{lo})}{\dot{z}_{td}-\dot{z}_{lo}} : (0,\ T_f) \mapsto (-1,\ 1) \\ \eta_s = & \quad \tfrac{2}{T_s} t : (-T_s/2,\ T_s/2) \mapsto (1,\ -1), \end{aligned}$$

where T_f and T_s refer to the flight and stance times and "*td*"and "*lo*" to touchdown and lift-off events.

Forward Speed Control: To run on the treadmill the robot has to adapt its relative speed to the treadmill and maintain its position at the center. Let the treadmill speed be $\dot{x}_{tread}$, and $\dot{x}$ be the absolute velocity of the robot, then the relative speed of the robot with respect to the treadmill will be $\dot{x}_{rel} = \dot{x} + \dot{x}_{tread}$. The objective is to maintain $x_d = \dot{x}_d = 0$. Therefore, the forward speed controller, the *foot placement algorithm*, takes the form

$$x_{ft,td,d} = x^*_{ft,td} + K_x x + K_{\dot{x}}\dot{x},$$

where $x^*_{ft,td}$ is the neutral foot position, K_x and $K_{\dot{x}}$ are gains, and $\bar{\dot{x}}_{rel}$ is the average relative velocity. The neutral touchdown foot position, $x^*_{ft,td}$, can be found using our previous results on passive dynamics via $x^*_{ft,td} = -r\sin\theta^*_{td}$, where $\theta^*_{td} = \hat{\theta}^*\sin((1-\rho)\pi)$ is the neutral touchdown angle, r is the leg length, and the neutral amplitude of oscillations (see [1] for details) is

$$\hat{\theta}^* = -\frac{\arcsin(T_s\bar{\dot{x}}_{rel}/2r_0)}{\sin((1-\rho)\pi)},$$

where r_0 is the leg length at rest and $\rho = T_s/(T_s+T_f)$ is the duty factor.

Leg Angle Tracking: During flight, the desired leg angle is derived as a function of locomotion variable $\theta_d(\eta) = \hat{\theta}_d\sin(\pi(1-\rho)\eta)$ and tracked via a model based controller which uses a simplified dynamical robot model. Controller design can be further simplified assuming the hip actuator bandwidth is much higher than the required leg oscillation frequencies. This allows for controller design decoupling. First, the controller derives $p_{h,d}$ trajectory, which is required to track our known trajectory $\theta_d(\eta)$. Second, The actuator tries to track the calculated $p_{h,d}$. Figure 3 illustrates the overall forward speed controller and the decoupled control actions.

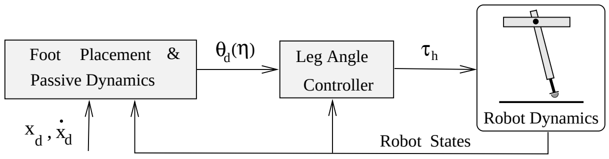

Figure 3: Forward speed controller.

The model based controller can result in a desirable actuator error equation $\ddot{e}_h + K_v\dot{e}_h + K_p e_h = 0$, where $e_h = p_{h,d} - p_h$. Similarly, $\ddot{e}_\theta + K_v{}'\dot{e}_\theta + K'_p e_\theta = 0$, where $e_\theta = \theta_d - \theta$. Finally, the hip controller can be found as

$$\tau_h = \alpha_h\left[\ddot{p}_{h,d} + K_v\dot{e}_h + K_p e_h\right] + r_h k_h\left[p_h + R(\theta-\phi)\right],$$

and

$$p_{h,d} = -R(\theta-\phi) - \frac{J_l}{Rk_h}\left[\ddot{\theta}_d + K'_v\dot{e}_\theta + K'_p e_\theta\right],$$

where k_h, r_h are the hip spring stiffness and ball screw lead, the K's are the gains, J_l the leg inertia about the hip, and $\alpha_h = J_s/r_h^2$ is a constant in terms of hip motor and screw inertia of J_s.

Body Pitch Control: The desired body pitch

$$\phi_d(\eta) = \hat{\phi}_d\sin(\pi\rho\eta),$$

is controlled during the stance; η is the stance locomotion time, and $\hat{\phi}_d = -J_b/J_l\hat{\theta}_d$ is the desired amplitude for body pitch oscillations. The derivation of the model based controller during stance is similar to the one during flight described above, and is presented in more detail in [11].

4 Experimental Results

It is important to study the robot's behavior both in transient and steady states. The steady–state experiments are needed to study the energetics of the robot, while the transient performance demonstrates the robustness of the controller under varying input velocities.

Figure 4 shows a running experiment which starts with vertical hopping ($\dot{x}_{tread} = 0$), ramps up to $1m/s$, maintains the maximum speed, and ramps down to zero speed vertical hopping again. Figure 5 shows that the vertical controller performs well in controlling the added energy and hopping height. The vertical controller, in the presence of the forward motion, still results in a stable and accurate hopping height control as shown in the lower plot of Figure 5.

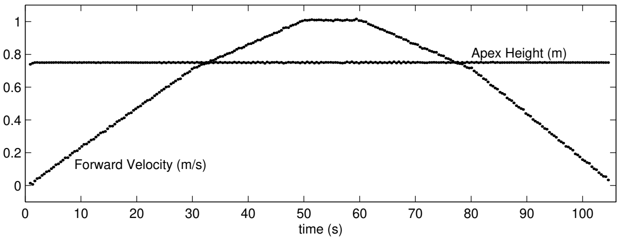

Figure 4: *Apex height and forward velocity. Height accuracy of* $\pm 0.005m$ *and forward position accuracy of* $\pm 0.03m$ *were achieved.*

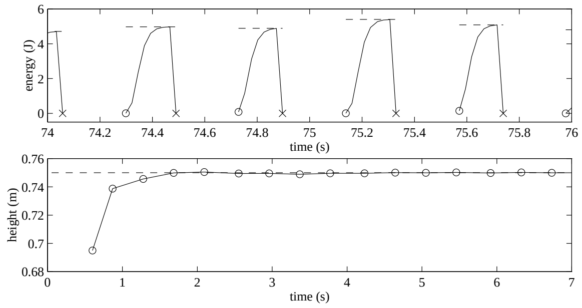

Figure 5: Top: Desired (dashed) and actual (solid) added energy. Bottom: The hopping height

4.1 Energetics

A conservative measure of energy expenditure is the integral of the absolute value of the instantaneous "shaft power,"

$$E = \int_{t_0}^{t_1} |\tau\omega| dt$$

where τ and ω are the torque and the angular velocity of the motor. This measure assumes that the actuator cannot gain energy from the system; as a result a higher estimate (conservative) of the actual mechanical energy is reported here. For our investigation, we will find it useful to examine the contributions of the hip and leg motors during flight and stance separately while the total energy expenditure of the robot is the sum of all four components. Note that this measure

Robot	*Motor*	*Stance*	*Flight*	Total
ARL Monopod (I)	*Leg*	$13J$	$12J$	$25J$
	Hip	$5J$	$20J$	$25J$
ARL Monopod (II)	*Leg*	$5J$	$5.5J$	$10.5J$
	Hip	$3.7J$	$6.5J$	$10.2J$

Table 1: *ARL Monopod I: Energy cost of* $50J$ *per step at* $1.2m/s$. *ARL Monopod II: Energy cost of almost* $20.7J$ *per step at* $1.25m/s$. *Shows more than* 50% *saving at almost the same speed.*

does not include the motor efficiency of converting input electric power to shaft power.

Energetics at Constant Speed: We have summarized the energetics of ARL Monopod II and ARL Monopod I in Table 1. Figure 6 shows how the energy is consumed during stance, flight, and a whole step. Compared to the energetics of the ARL Monopod I [7], where the body pitch controller consumed $5J$ and the forward speed controller consumed $20J$ (at $1.2m/s$), dramatic reductions are achieved: The saving amounts to approximately 67% for the forward speed controller and about 26% for the pitch angle controller. In addition, some savings are obtained for the leg motor. For both flight and stance savings are more than 50%. The total energy has dropped from $50J/step$ to less than $20J/step$, which means 58% energy savings. Considering that the ARL Monopod II is also heavier ($18kg$) than the ARL Monopod I ($15kg$), the improvements in efficiency are higher.

Specific Resistance: A fair measure of efficiency of a mobile robot should account for the weight and velocity of the robot. A general measure was introduced by Gabrielli and von Kármán [12], defined by

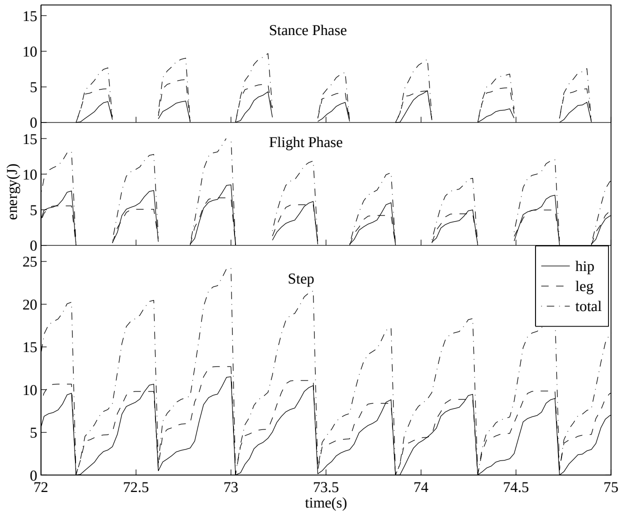

Figure 6: *Energetics at* $1.25m/s$*.*

$\varepsilon = P/(mgv_{max})$, called "Specific Resistance." P is the output power, mg the total weight and v_{max} is the maximum speed. This measure with a slight change is used to express ε at different speeds as $\varepsilon(\dot{x}) = \frac{P(\dot{x})}{mg\dot{x}}$. The total output power for our robot at maximum speed is $P = 20.7J/step \cdot 2.3steps/s \approx 48W$. Comparing the ARL Monopod II, which has,

$$\varepsilon_{II} = \frac{48W}{18kg \cdot 9.81m/s^2 \cdot 1.25m/s} \approx 0.22$$

with the ARL Monopod I, which has,

$$\varepsilon_{I} = \frac{125W}{15kg \cdot 9.81m/s^2 \cdot 1.2m/s} \approx 0.7$$

shows almost a 70% improvement. The drastic change in ε is partially due to the higher weight, but is mostly due to the energy savings.

Forward Velocity Effects: The energy expenditure of the robot is a function of the velocity. The leg energy, Figure 7 (a), shows a gradual increase at lower speeds but an abrupt change is observed at higher speeds. The hip energy per step increases almost linearly with velocity, as illustrated in Figure 7 (b). This behavior matches the trend of the simulation results of passive dynamics running of [1]. Figure 7 (c) shows the total energy expenditure of the system per step. The curve for specific resistance ε, Figure 7 (d), shows a very low efficiency (high ε) at low speeds, due to the "overhead" energy spent to maintain the vertical motion, which does not contribute to the forward motion. The ε curve is almost flat for speeds between $0.9m/s$ and $1.25m/s$. This can be attributed to practical limitations such as increased damping forces which are proportional to the square of the velocity.

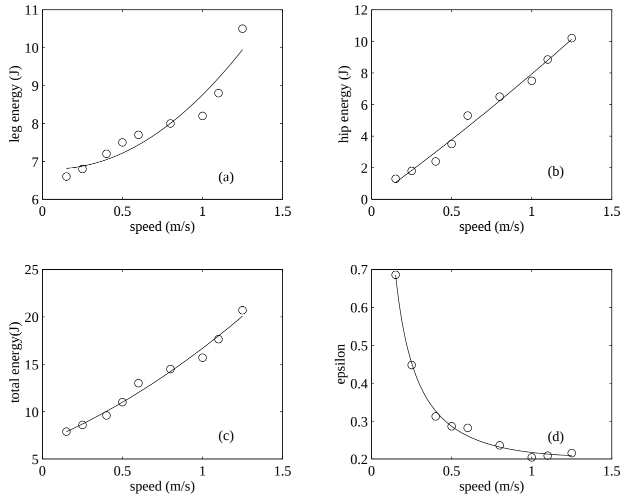

Figure 7: *In the first three curves "○" represents an actual data point and the solid curves are a second order curve fit. (a) The leg motor energy per step. (b) The hip motor energy per step. (c) The total energy per step. (d) Specific resistance (ε).*

The overall change in specific resistance as a function of velocity can be understood based on a few simple but fundamental facts. Consider the power consumption at zero speed, the "overhead power," to be $P(0)$, and assume that power loss is of the form $P(\dot{x}) = \alpha\dot{x}^2 + \beta\dot{x}$, where $\alpha(N)$ and $\beta(Ns/m)$ are to be identified. This relationship is based on the fact that the vertical energy per step is well fit with a quadratic curve and hip energy per step with a line (see Figure 7). The power, as we saw earlier, can be easily related to the energy per step. Therefore, the specific resistance is calculated by

$$\varepsilon(\dot{x}) = \frac{P(0) + \alpha\dot{x}^2 + \beta\dot{x}}{mg\dot{x}}, \tag{1}$$

where α is a constant. Such a curve has a minimum at $\dot{x}_{opt} = (P(0)/\alpha)^{\frac{1}{2}}$, where $d\varepsilon/d\dot{x} = 0$. Since $P(0) > 0$ and $\alpha > 0$, the minimum value always exists and is

$$\varepsilon_{opt} = \varepsilon(\dot{x}_{opt}) = \frac{2\sqrt{\alpha P(0)} + \beta}{mg}.$$

For the ARL Monopod II, $P(0) = 15.6W$, but we do not have data for speeds above $1.25m/s$; therefore, the speed of minimum ε was not identified. But the trend of the curve in Figure 7 shows that we are very close to the minimum. The curve shows that the optimum is almost at $\dot{x}_{opt} = 1.4m/s$, and its value is $\varepsilon_{opt} \approx 0.21$

from the curve (d) in Figure 7. Thus, $\alpha \approx 8.0$, $\beta \approx 14.8$ and

$$\varepsilon(\dot{x}) = \frac{15.6W \ + \ 8(Ns/m) \cdot \dot{x}^2 \ + \ 14.8(N) \cdot \dot{x}}{18(kg) \cdot 9.81(m/s^2) \cdot \dot{x}}. \quad (2)$$

The above calculations were given only as an example to predict the behavior of ε at higher speeds, which were not attainable by experiments.

Finally, Figure 8 shows the specific resistance for selected machines and human activities. Except for ARL Monopod II, the curves are all borrowed from [7], which includes a brief survey of machines and human energetics. From this graph it is clear that the ARL Monopod II has achieved a far greater energy efficiency than any other actively controlled legged robot. The dashed segment of the curve for ARL Monopod II is based on the predicted behavior (2) at higher speeds.

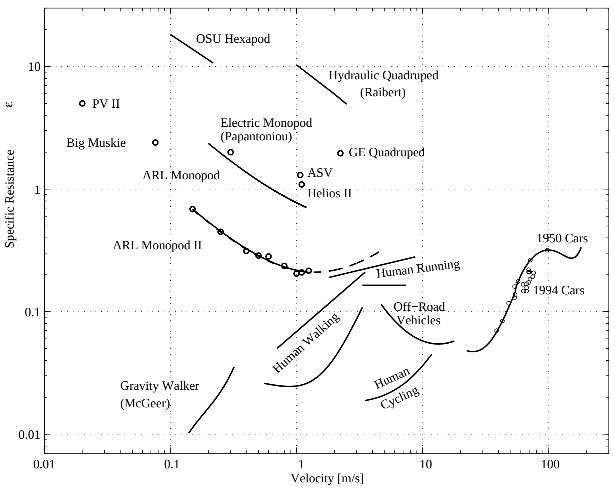

Figure 8: *Specific Resistance for selected land vehicles and human running.*

Summary

The experimental implementation of Controlled Passive Dynamic Running strategy on the ARL Monopod II was presented. A simple adaptive and energy-based controller stabilized the vertical motion with a very high accuracy. Subsequently, several vertical and forward running experiments were performed with the robot and a top speed of $4.5km/h$ was achieved. Implementation of Controlled Passive Dynamic Running showed dramatic reductions in the energy consumption of the ARL Monopod II, compared to ARL Monopod I that has no hip compliance. The specific resistance was reduced approximately by 70%. A diagram illustrating the specific resistance in terms of forward speed was used to compare the efficiency of our robots to biological locomotion, wheeled vehicles, and other legged robots.

References

[1] M. Ahmadi and M. Buehler, "Stable control of a simulated one-legged running robot with hip and leg compliance", *IEEE Trans. Robotics and Automation*, vol. 13, no. 1, pp. 96–104, Feb 1997.

[2] M. Ahmadi and M. Buehler, "Preliminary experiments with an actively tuned passive dynamic running robot", in *Experimental Robotics V*, pp. 249–260. Springer-Verlag, 1997.

[3] N. J. Dimery et al., "Elastic extension of leg tendons in the locomotion of horses", *J. Zoology*, vol. 210, pp. 415–425, 1986.

[4] M. H. Raibert, *Legged Robots That Balance*, MIT Press, Cambridge, MA, 1986.

[5] K. Matsuoka, "A mechanical model of repetitive hopping movements", *Biomechanisms*, vol. 5, pp. 251–258, 1980.

[6] K. V. Papantoniou, "Electromechanical design for an electrically powered, actively balanced one leg planar robot", in *Proc. IEEE/RSJ Int. Conf. Intelligent Systems and Robots*, Osaka, Japan, 1991, pp. 1553–1560.

[7] P. Gregorio, M. Ahmadi, and M. Buehler, "Design, control and energetics of an electrically actuated legged robot", *IEEE Trans. Systems, Man, and Cybernetics*, vol. 27, no. 4, pp. 626–634, Aug 1997.

[8] A. Lebaudy, J. Prosser, and M. Kam, "Control algorithms for a vertically-constrained one-legged hopping machine", in *Proc. IEEE Int. Conf. Decision and Control*, 1993, pp. 2688–2693.

[9] T. McGeer, "Passive dynamic walking", *Int. J. Robotics Research*, vol. 9, no. 2, pp. 62–82, 1990.

[10] M. H. Raibert and C. M. Thompson, "Passive dynamic running", in *Experimental Robotics I*, V. Hayward and O. Khatib, Eds., pp. 74–83. Springer-Verlag, NY, 1989.

[11] M. Ahmadi, *Stable Control of a One-Legged Robot Exploiting Passive Dynamics*, PhD thesis, McGill, March 1998.

[12] G. Gabrielli and T. H. von Karman, "What price speed?", *Mechanical Engineering*, vol. 72, no. 10, pp. 775–781, 1950.